

# Proof of principle for a molecular 1 : 2 demultiplexer to function as an autonomously switching theranostic device<sup>c</sup>

Cite this: *Chem. Sci.*, 2013, **4**, 858

Sundus Erbas-Cakmak,<sup>a</sup> O. Altan Bozdemir,<sup>c</sup> Yusuf Cakmak<sup>a</sup> and Engin U. Akkaya<sup>\*ab</sup>

Received 11th September 2012  
Accepted 16th October 2012

DOI: 10.1039/c2sc21499g

[www.rsc.org/chemicalscience](http://www.rsc.org/chemicalscience)

Guided by the digital design concepts, we synthesized a two-module molecular demultiplexer (DEMUX) where the output is switched between emission at near IR, and cytotoxic singlet oxygen, with light at 625 nm as the input (I), and acid as the control (c). In the neutral form, the compound fluoresces brightly under excitation at 625 nm, however, acid addition moves the absorption bands of the two modules in opposite directions, resulting in an effective reversal of excitation energy transfer direction, with a concomitant upsurge of singlet oxygen generation and decrease in emission intensity.

## Introduction

Ever since the seminal de Silva article was published in 1993,<sup>1</sup> chemical logic gate research is in a process of rapid progress and evolution. Now closing in on its second decade, chemical equivalents of many two input logic gates were reported,<sup>2</sup> along with more complex digital systems featuring higher levels of virtual integration.<sup>3</sup> Finding tangible applications for these molecular constructs with digital capabilities has been in the forefront of research in recent years.<sup>4</sup> Progress in this field was essentially based on the premise that for molecular logic gates, while getting their inspiration from their silicon based counterparts in digital electronics, the limitations and potential opportunities do not necessarily show a one-to-one correspondence. The often stated limitation of “input–output heterogeneity” can be molded into a distinct advantage, since the outputs can be molecular in nature which may interact with other, and more complex molecular and supramolecular phenomena such as metabolism, thus opening a new path to information processing therapeutic agents.<sup>5</sup> In addition, certain design flexibilities available in molecular logic gates, have no counterparts in semiconductor based analogues. Functional/virtual integration of logic gates and possibility of superposed logic gates are just two examples. These two uniquely molecular features are exploited in a typical design of molecular multiplexers<sup>6</sup> (MUX) and demultiplexers<sup>7</sup> (DEMUX). In digital signal

processing, a multiplexer is a combinatorial circuit which selects from a number of inputs and directs it to an output. A demultiplexer is a complementary device, taking a single input signal and switching it between multiple output signals. Both can be considered as controlled switches.<sup>8</sup>

Previously, we have shown<sup>4a</sup> that even a simple AND logic gate within the context of photodynamic therapy can bring in highly precious surplus value of enhanced selectivity. Photodynamic therapy is a non-invasive methodology of treatment for various cancers and non-cancerous indications.<sup>9</sup> This methodology is based on the excitation of a particular photosensitizer within the tumor tissue, generating singlet oxygen and other reactive oxygen species (ROS), and thus, regiospecifically destroying the targeted tumor. In recent years, combined diagnosis and therapy functions received particular attention, with a new buzz word to accompany this heightened interest: theranostics. The diagnosis component obviously includes, but is not limited to imaging of the region of interest. As for therapeutic methodologies, such multifunctional delivery agents would be useful for photodynamic therapy as well.

It occurred to us that a molecular DEMUX device, which can switch between two outputs such as light and cytotoxic singlet oxygen can be very useful in a photodynamic theranostics context. Such a molecular device when directed to the tumor region, may fluoresce brightly in the surrounding healthy tissue, and inside the tumor, appear dark while generating singlet oxygen on excitation. The switch can be made by the acidity difference between the tumors and the healthy tissue without any need to change the wavelength of excitation. It is widely known that most tumors are considerably acidic compared to neighbouring healthy tissues as a result of the Warburg effect.<sup>10</sup> If the design is made properly, the emission can be at the red or near IR region of the spectrum making imaging more valuable.

<sup>a</sup>UNAM-Institute of Materials Science and Nanotechnology, Bilkent University, Ankara, 06800, Turkey. E-mail: eua@fen.bilkent.edu.tr; Fax: +90 312-266-4068; Tel: +90 312-290-2450

<sup>b</sup>Department of Chemistry, Bilkent University, Ankara, 06800, Turkey

<sup>c</sup>Department of Chemistry, Ataturk University, Erzurum, 25240, Turkey

† Electronic supplementary information (ESI) available: General information about synthesis and measurements, absorbance and excitation spectra, singlet oxygen generation experiments, synthetic details, NMR and mass spectra of synthesized compounds. See DOI: 10.1039/c2sc21499g

## Results and discussion

With these goals in mind, we designed a proof-of-principle DEMUX, which can operate in organic solvents, incorporating switchable through space energy transfer coupled to mutually exclusive generation of red/near IR fluorescence emission or singlet oxygen generation depending on the acidity of the medium. Here, the light at 625 nm (supplied by a LED array) is the input (I), and the acid (trifluoroacetic acid, TFA) is the control (or address input). The target molecule is composed of two distyryl-Bodipy modules clicked together by Huisgen cycloaddition (Scheme S1<sup>†</sup>). Our previous experience with distyryl-Bodipys<sup>11</sup> taught us that pyridylethenyl and dimethylaminophenylethenyl substituted Bodipys respond by opposite spectral shifts on protonation (blue shift with dimethylaminophenyl, and red shift with pyridyl) as a result of different internal charge transfer (ICT) characteristics. When excited at a fixed wavelength, it is reasonable to expect a switch in the direction of energy transfer (Fig. 1, 2 and S1<sup>†</sup>). Furthermore, one of the Bodipy modules (2, FL module) is designed to be fluorescent, and especially more so on protonation. The other one (1, the PS module) carries heavy atoms (two iodine atoms at 2,6-positions) facilitating intersystem crossing to yield a higher rate of singlet oxygen generation. It is clear that the switch is not going to be absolute, *i.e.*, both modules will be excited at varying degrees, nevertheless an inspection of Fig. 2 reveals that at the optimal wavelength (635 nm), the PS to FL absorptivity ratio changes from 2 to 0.5, altering the position of preferential initial excitation.

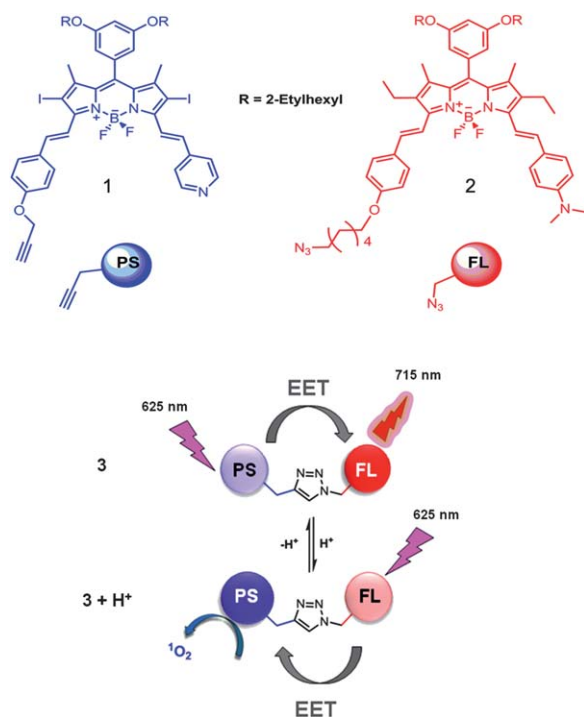


**Fig. 1** Modular assembly of the molecular DEMUX device with two different outputs depending on the acidity of the medium.

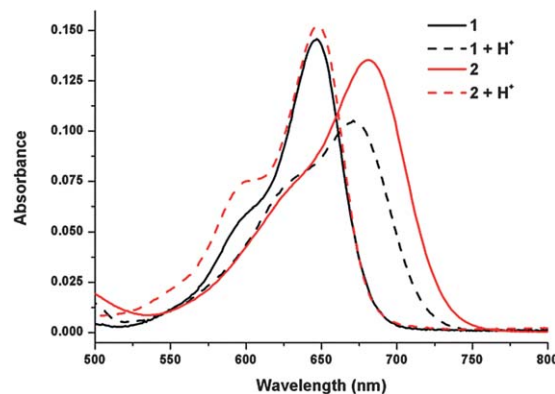


**Fig. 2** Absorbance spectra of equal concentrations (2  $\mu\text{M}$ ) of the photosensitizer (PS, **1**) and the fluorophore (FL, **2**) modules in the presence (dashed curves) and absence (solid curves) of added TFA in chloroform.

The operation of the DEMUX can be broken down into superposed action of two modules clicked together. Compound **3** shows a broad band and it is difficult to assess spectral changes on the addition of control input TFA (Fig. S1<sup>†</sup>). But, when the two components are separately studied as independent modules, the operation of compound **3** can be better understood. When no acid is added, maximum absorbance of the isolated PS module (**1**) is at 647 nm and that of the FL module (**2**) is at 681 nm, however, when TFA is added, the absorption peak of **1** shifts to 671 nm, whereas that of **2** shifts to 647 nm (Table 1 and Fig. 2). An opposite shift is also observed in emission spectra of modules **1** and **2** (Fig. S1<sup>†</sup>). While the difference seems to be small, adding the auxochromic nature of the protonation of **2**, it should not be surprising to see that the compound **3** works in accordance with the design expectations. For compound **3**, when there is no added acid ( $c = 0$ ), on excitation at 625 nm, an intense emission at 715 nm from the FL module is observed in accordance with the operation of the DEMUX device corresponding to input  $h\nu_{625} = 1$ ,  $c = 0$ ; therefore output is switched to output 1, which is  $h\nu_{715}$ . Here, we took advantage of the faster rate of the excited state energy transfer process with respect to intersystem crossing<sup>12</sup> to quench the singlet oxygen generation near neutral pH and yield near IR emission instead (*vide infra*).

**Table 1** Photophysical characterization of compounds **1**, **2** and **3** in chloroform

Compound	$\lambda_{\text{abs}}$ [nm]	$\epsilon$ [ $\text{M}^{-1} \text{cm}^{-1}$ ]	$\lambda_{\text{F}}$ [nm]	$\phi_{\text{F}}^a$ [ $\lambda_{\text{exc}}$ (nm)]	$\tau_{\text{F}}^b$ [ns]
<b>1</b>	647	73 000	665	0.22	1.71
<b>1</b> + $\text{H}^+$	671	53 000	694	0.06	0.33
<b>2</b>	681	68 000	729	0.16	3.37
<b>2</b> + $\text{H}^+$	647	76 000	665	0.41	3.62
<b>3</b>	652	121 000	715	0.42	4.05
<b>3</b> + $\text{H}^+$	650	105 000	700	0.02	0.03

<sup>a</sup> Quantum yields were calculated using Sulforhodamine 101 (excitation at 550 nm, in EtOH) as reference. All other compounds were dissolved in chloroform. <sup>b</sup> All measurements are taken in  $\text{CHCl}_3$  using 650 nm (for compounds **1** and **2**) and 667 nm (for compound **3**) NanoLEDS.

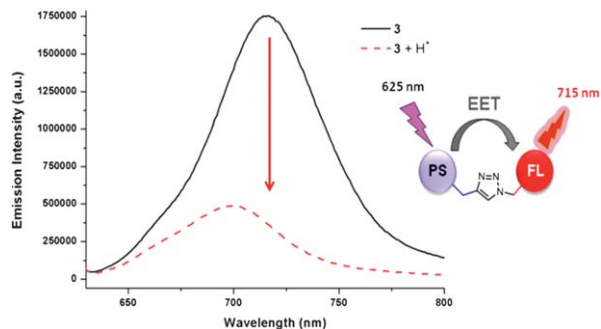


**Fig. 3** Emission spectra of the DEMUX device **3**, under neutral (black, solid) and acidic (red, dashed) conditions excited at 625 nm in chloroform.

Excitation energy transfer (EET) from the PS to FL in DEMUX compound **3** is confirmed by the decrease in the singlet oxygen generation capacity of the PS module (ESI, Table S1, Fig. S2 and S3<sup>†</sup>), even though it actively generates  $^1\text{O}_2$  when that module alone was excited separately, both under acidic and neutral conditions (ESI, Fig. S2 and S3<sup>†</sup>). On acid addition, ( $c = 1$ ) and excitation at the fixed wavelength of 625 nm, simultaneous ICT shifts in PS and FL change the direction of EET and cytotoxic singlet oxygen is then produced, while the emission of FL is quenched (Fig. 3). Energy transfer to the PS module in compound **3** is also confirmed by the decrease in the excited state lifetime of protonated compound **3** (0.03 ns,  $\chi^2 = 1.43$ ) compared to the protonated donor FL module (3.62 ns,  $\chi^2 = 1.21$ ) in  $\text{CHCl}_3$ , indicating a very high energy transfer efficiency (99%).

Three negative and two positive control experiments support the mutually exclusive character of near IR fluorescence emission and singlet oxygen generation (Table 2). In positive controls, the singlet oxygen generation activity of 20 nM compound **1** (PS module, same concentration as the demultiplexer **3**) was studied, and as expected, found to be high, both in the presence or absence of trifluoroacetic acid (ESI, Fig. S2 and S3<sup>†</sup>). This shows that the decrease in the singlet oxygen generation rate is mostly due to the presence of the fluorophore module as an energy sink. The relative singlet oxygen generation efficiencies were calculated by normalizing the rate of initial decrease in the DPBF degradation/bleaching (ESI<sup>†</sup>). In

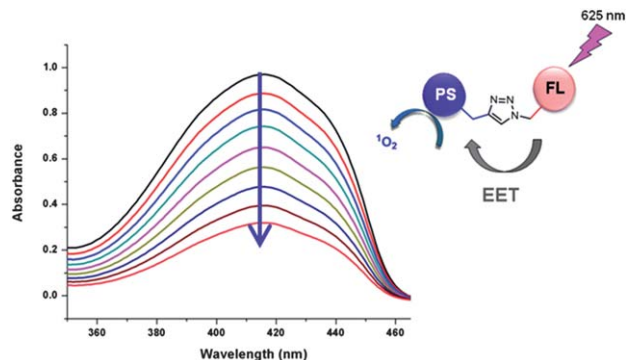


**Fig. 4** Singlet oxygen mediated photobleaching of DPBF (50  $\mu\text{M}$ ) in the presence of 20 nM compound **3** and TFA (20  $\mu\text{L}/3 \text{ mL}$ ) in chloroform.

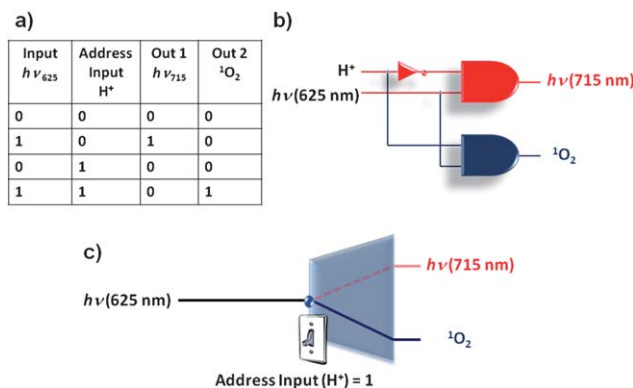


**Fig. 5** Truth table (a), circuit diagram (b) and schematic switching operation (c) of the 1 : 2 molecular DEMUX logic device.

the case of **1** (PS) alone (positive control-1), the efficiency seems to decrease to 0.56 compared to compound **3** under acidic conditions.

This is probably due to the larger absorptivity of the protonated FL unit which leads to excitation of the PS in **3** by EET. The PS under acidic conditions exhibits a decrease in the rate of  $^1\text{O}_2$  generation which is due to the decrease in molar absorptivity at the wavelength of excitation (625 nm) as a result of the bathochromic shift on protonation. In addition, by using

**Table 2** Experimental data for the generation of photonic and chemical outputs in response to the input acted by the address switch

Compound	Irradiation (625 nm)	$\text{H}^+$ (address input)	Relative emission intensity (715 nm)	Relative $^1\text{O}_2$ generation efficiency <sup>a</sup>
<b>3</b>	0	0	0	0
<b>3</b>	1	0	1	0.14
<b>3</b>	0	1 <sup>b</sup>	0	<0.01
<b>3</b>	1	1 <sup>b</sup>	0.21	1.0
<b>1</b>	0	0	—	0
<b>1</b>	1	0	—	1
<b>1</b>	0	1	—	<0.01
<b>1</b>	1	1	—	0.56

<sup>a</sup> Relative singlet oxygen generation was calculated by setting the rate of DPBF degradation at input = 1, address = 1 case to be 1. <sup>b</sup> 20  $\mu\text{L}$  TFA was added to 3 mL of each sample. Details of calculations were given in the ESI<sup>†</sup>.

two negative controls, it was shown that there is no degradation of the trap molecule (diphenylisobenzofuran, DPBF) in the absence of photosensitizer under neutral and acidic conditions (ESI, Fig. S2 and S3†). The third negative control was carried out to determine the extent of singlet oxygen generation of compound **3** under neutral conditions, *i.e.*, in the absence of added acid. In this experiment, due to effective reversed EET from the **PS** to **FL**, no singlet oxygen generation is observed as expected (Table 2 and S2†).

Furthermore, control experiments with trap alone were performed to ensure the reliability of the data. In acidic conditions, reciprocal shifts in the absorbance of the two modules of the compound **3** lead to a change in the direction of EET. The **2** (**FL**) becomes the donor, and excitation energy is transferred to **1** (**PS**), which becomes activated and generates cytotoxic singlet oxygen effectively at concentrations as low as 20 nM (Fig. 4 and 5). The response of compound **3** and all other control experiments under neutral and acidic conditions in dark and under red LED irradiation at 625 nm is shown in Table 2.

The overall working principle of the compound presented here as a molecular DEMUX device is as follows; in the absence of acid, there is an intense emission near IR at around 715 nm (Fig. 3). When the acid is added, the fluorescence of the compound **3** is completely quenched due to EET to the non-emissive PS module. This decrease in emission is linked to the efficient generation of singlet oxygen. With the pH-driven change in the EET direction, the **PS** module becomes active and generates therapeutic output, singlet oxygen. This action is dependent on the change in EET direction, thus, with a similar demultiplexer based on this proof of principle, but with additional practical considerations in mind (solubility, pK<sub>a</sub> values of the acid sensitive groups), sensitization to produce singlet oxygen would be only in the acidic medium (as found in most tumors) and the boundaries of the tumor region can be imaged by the change in fluorescence intensity (which would appear as darker regions, as opposed to red/near IR fluorescence from the surrounding healthy tissues).

The demultiplexer device described in this work acts reversibly and retains most of its fluorescence intensity even after 5 cycles of pH oscillations (ESI, Fig. S4†).

## Conclusions

The importance of multifunctional drugs and delivery systems is well appreciated, and in this work, we demonstrated that the two critical functions, *i.e.*, diagnostic and therapeutic actions can be in principle, implemented using a single molecular agent. We expect this proof of principle model of a demultiplexer to pave the way to multifunctional molecular systems, which would interactively deliver the therapeutic agent, while offering diagnostic imaging possibilities. It is obvious that the water solubility issue has to be addressed, and the molecular device would be even more valuable if it could be transformed into another one where the emission in the tumor region is turned on. Regardless, the idea seems to be perfectly transferable to other designs where the practical issues as mentioned above could be addressed. The work described here suggests

that even at a relatively rudimentary stage, information processing molecules can produce unprecedented capabilities, such as autonomous decision making to switch between diagnostic and therapeutic modes. And this is made possible by a unimolecular superposed logic operation with no semiconductor counterpart. The future of molecular logic gate research looks very bright.

## Acknowledgements

We are grateful for funding by the National Boron Research Institute (BOREN), Turkish Academy of Sciences (TUBA). Additional funding from TUBITAK is gratefully acknowledged. S.E.-C. thanks TUBITAK and Y.C. thanks UNAM for scholarships.

## Notes and references

- 1 A. P. de Silva, N. H. Q. Gunaratne and C. P. McCoy, *Nature*, 1993, **364**, 42.
- 2 (a) A. Credi, *Angew. Chem., Int. Ed.*, 2007, **46**, 5472; (b) K. Szacilowski, *Chem. Soc. Rev.*, 2008, **108**, 3481.
- 3 (a) U. Pischel, *Angew. Chem., Int. Ed.*, 2007, **46**, 4026; (b) A. P. de Silva and N. D. McClenaghan, *Chem.-Eur. J.*, 2002, **8**, 4935; (c) F. Remacle, S. Speiser and R. D. Levine, *J. Phys. Chem. B*, 2001, **105**, 5589; (d) S. J. Langford and T. Yann, *J. Am. Chem. Soc.*, 2003, **125**, 11198; (e) R. Guliyev, S. Ozturk, Z. Kostereli and E. U. Akkaya, *Angew. Chem., Int. Ed.*, 2011, **50**, 9826; (f) O. A. Bozdemir, R. Guliyev, O. Buyukcakir, S. Selcuk, S. Kolemen, G. Gulseren, T. Nalbantoglu, H. Boyaci and E. U. Akkaya, *J. Am. Chem. Soc.*, 2010, **132**, 8029; (g) A. Coskun, E. Deniz and E. U. Akkaya, *Org. Lett.*, 2005, **7**, 5187; (h) D. Margulies, G. Melman and A. Shanzer, *Nat. Mater.*, 2012, **4**, 768; (i) D. Margulies, G. Melman and A. Shanzer, *J. Am. Chem. Soc.*, 2006, **128**, 4865; (j) D.-H. Qu, Q.-C. Wang and H. Tian, *Angew. Chem.*, 2005, **117**, 5430; (k) G. de Ruiter, L. Motiei, J. Choudhury, N. Oded and M. E. van der Boom, *Angew. Chem., Int. Ed.*, 2010, **49**, 4780; (l) G. de Ruiter, E. Tartakovski, N. Oded and M. E. van der Boom, *Angew. Chem., Int. Ed.*, 2010, **49**, 173; (m) M. Semeraro and A. Credi, *J. Phys. Chem. C*, 2010, **114**, 3209; (n) L. Zhang, W. A. Whitfield and L. Zhu, *Chem. Commun.*, 2008, 1880; (o) S. Kou, H. N. Lee, D. van Noort, K. M. K. Swamy, S. H. Kim, J. H. Soh, K.-M. Lee, S.-W. Nam, J. Yoon and S. Park, *Angew. Chem., Int. Ed.*, 2008, **47**, 872; (p) P. Ceroni, G. Bergamini and V. Balzani, *Angew. Chem., Int. Ed.*, 2009, **48**, 8516; (q) T. Gupta and M. E. van der Boom, *Angew. Chem.*, 2008, **120**, 5402.
- 4 (a) S. Ozlem and E. U. Akkaya, *J. Am. Chem. Soc.*, 2009, **131**, 48; (b) D. C. Magri, G. J. Brown, G. D. McClean and A. P. de Silva, *J. Am. Chem. Soc.*, 2006, **128**, 4950; (c) A. P. de Silva and S. Uchiyama, *Nat. Nanotechnol.*, 2007, **2**, 399–410; (d) V. Balzani, A. Credi and M. Venturi, *ChemPhysChem*, 2003, **4**, 49; (e) D. Margulies, C. E. Felder, G. Melman and A. Shanzer, *J. Am. Chem. Soc.*, 2007, **129**, 347; (f) S. Angelos, Y.-W. Yang, N. M. Khashab, J. F. Stoddart and J. I. Zink, *J. Am. Chem. Soc.*, 2009, **131**, 11344; (g) U. Pischel, *Angew. Chem., Int. Ed.*, 2010, **49**, 1356.

- 5 (a) M. N. Win and C. D. Smolke, *Science*, 2008, **322**, 456; (b) X. Chen, Y. Wang, Q. Liu, Z. Zhang, C. Fan and L. He, *Angew. Chem., Int. Ed.*, 2006, **45**, 1759; (c) R. J. Amir, M. Popkov, R. A. Lerner, C. F. Carbas III and D. Shabat, *Angew. Chem., Int. Ed.*, 2005, **44**, 4378; (d) J. Szacilowski, *BioSystems*, 2007, **90**, 738; (e) T. Niazov, R. Baron, E. Katz, O. Lioubashevski and I. Willner, *Proc. Natl. Acad. Sci. U. S. A.*, 2006, **103**, 17160.
- 6 J. Andreasson, S. D. Straight, S. Bandyopadhyay, R. H. Mitchell, T. A. Moore and D. Gust, *Angew. Chem., Int. Ed.*, 2007, **46**, 958.
- 7 (a) M. Amelia, M. Baroncini and A. Credi, *Angew. Chem., Int. Ed.*, 2008, **47**, 6240; (b) E. Perez-Inestrosa, J.-M. Montenegro, D. Collado and R. Suau, *Chem. Commun.*, 2008, 1085.
- 8 (a) F. Raymo, *Adv. Mater.*, 2002, **14**, 401; (b) V. V. Zhirnov, R. K. Cavin, J. A. Hutchby and G. I. Bourianoff, *Proc. IEEE*, 2003, **91**, 1934.
- 9 T. J. Dougherty, C. J. Gomer, B. W. Henderson, G. Jori, D. Kessel, M. Korbelik, J. Moan and Q. Peng, *J. Natl. Cancer Inst.*, 1998, **90**, 889.
- 10 M. G. V. Heiden, L. C. Cantley and C. B. Thompson, *Science*, 2009, **324**, 1029.
- 11 E. Deniz, G. C. Isbasar, O. A. Bozdemir, L. T. Yildirim, A. Siemiarzuck and E. U. Akkaya, *Org. Lett.*, 2008, **10**, 3401.
- 12 J. F. Lovell, J. Chen, M. T. Jarvi, W. G. Cao, A. D. Allen, Y. Liu, T. T. Tidwell, B. C. Wilson and G. Zheng, *J. Phys. Chem. B*, 2009, **113**, 3203.